IBIS
BOU international journal of avian science
Ibis (2024), **166**, 308–314 doi: 10.1111/ibi.13264

Short Communication

Variation in flight characteristics associated with entry by eagles into rotor-swept zones of wind turbines

BRIAN W. ROLEK,[1] MELISSA A. BRAHAM,[2] TRICIA A. MILLER,[2] ADAM E. DUERR[2] TODD E. KATZNER[3] & CHRISTOPHER J. W. MCCLURE*[1]
[1]*The Peregrine Fund, Boise, Idaho, USA*
[2]*Conservation Science Global, Cape May, New Jersey, USA*
[3]*U.S. Geological Survey, Boise, Idaho, USA*

Automated curtailment of wind turbines can reduce fatality rates of wildlife but the resulting increased number of curtailments can reduce power generation. Tailoring curtailment criteria for each individual turbine could reduce unnecessary curtailment, yet it is unknown whether the risk to wildlife varies among turbines. We demonstrate turbine-specific variation in the speed, altitude, approach angle and distance metrics associated with entry by eagles into rotor-swept zones. Our results thus illustrate the potential value of turbine-specific curtailment criteria to reduce fatality rates of wildlife at wind energy facilities.

Keywords: curtailment, eagle, rotor-swept zone, wildlife collision, wind energy, wind turbine.

Large soaring birds, including eagles and other raptors, are among the bird species most often found killed by wind energy infrastructure (Perold *et al.* 2020), yet there are methods to reduce fatalities at operating turbines (Marques *et al.* 2014). For example, individual wind turbines can be slowed or stopped (i.e. 'curtailed') in real-time when wildlife is considered at risk of collision (BirdLife International 2015, Allison *et al.* 2017). This process is commonly referred to as 'automated curtailment', 'shutdown on command' or 'smart curtailment' and is increasingly being implemented at wind-power facilities (C. J. W. McClure and T. E. Katzner pers. obs.).

Initial analyses have suggested that automated curtailment using the machine vision system 'IdentiFlight' (IdentiFlight International, Louisville, CO, USA) reduced the fatality rate of Bald Eagles *Haliaeetus leucocephalus* and Golden Eagles *Aquila chrysaetos* at a wind-power facility in Wyoming, USA (McClure *et al.* 2021b, 2022). However, this reduction in fatalities was concurrent with an increase in the frequency of curtailment (McClure *et al.* 2021b) and presumably also caused a decrease in power generation.

Automated curtailments at the Wyoming facility are currently triggered using a set of criteria based on the flight trajectories of birds that an artificial intelligence system classifies as eagles. These criteria are the same for all individual turbines within the facility (McClure *et al.* 2021a). However, risk to wildlife posed by individual wind turbines often varies within wind-power facilities (Smallwood *et al.* 2007, De Lucas *et al.* 2008, 2012). Indeed, many eagles that triggered curtailments at the Wyoming facility never entered the rotor-swept zone, the area where wildlife can collide with turbine blades (McClure *et al.* 2021a). Therefore, excess curtailment could be reduced if criteria could be developed to incorporate turbine-specific probabilities describing whether or not nearby eagles would enter the rotor-swept zone (McClure *et al.* 2021a).

Flight characteristics at the Wyoming facility have been shown accurately to forecast entry into the rotor-swept zone of a generic turbine (Rolek *et al.* 2022). However, it is unknown whether these characteristics vary among turbines, and we predicted that such variation exists. Our objective is to test this prediction. We modified the modelling framework presented by Rolek *et al.* (2022) to estimate the variation among turbines in flight characteristics associated with entry by eagles into the rotor-swept zone. Such information could help further improve curtailment criteria for automated curtailment by the machine vision system using in-flight characteristics to better predict an eagle's probability of entering the rotor-swept zone and potentially reduce excess curtailment.

METHODS

Study site

We evaluated flight characteristics of eagles at Top of the World, a wind-power facility operated by Duke Energy Renewables and located in Converse County, WY, USA (see fig. 1 McClure *et al.* 2021a, 2021b for map of the study area). This facility is composed of 66 General Electric 1.5-MW turbines with rotor diameters of 77 m, and 44 Siemens 2.3-MW turbines with rotor diameters of 101 m. All turbines had a hub height of 80 m.

*Corresponding author.
Email: cmcclure@peregrinefund.org
Twitter: @CJWMcClure

Automated monitoring system and curtailment

IdentiFlight is an automated monitoring system that tracks and identifies moving objects. It first uses a computer vision algorithm to classify moving objects within 1000 m as eagles or non-eagles. It then uses stereoscopic cameras to estimate locations of those objects identified as eagles in three-dimensional space at 200-ms intervals (5 frames per second). These estimated locations are aggregated to produce digitized representations of flight paths through the wind-power facility.

Forty-seven IdentiFlight units were incrementally installed at Top of the World from 18 May 2018 to 13 August 2019. Units were positioned to provide coverage for all turbines. At this site, IdentiFlight uses distance to turbine, estimated time to collision, an eagle's relative bearing in relation to the turbine and confidence that the bird was an eagle to determine whether curtailment should be implemented (McClure *et al.* 2021a). For additional details about IdentiFlight at this site, see McClure *et al.* (2018). We included IdentiFlight data collected between 18 May 2018 and 31 March 2019.

Flight characteristics

We considered five explanatory variables (i.e. flight characteristics) to predict probability of entry of an eagle into the rotor-swept zone. Each of the flight characteristics was associated with a single 5-s segment of a flight path and was averaged over that segment. Two of these characteristics were flight altitude (ALTITUDE) and speed of eagles (SPEED). We decomposed relative and compass bearings using standard methods for including circular data as explanatory variables in regressions (Crawley 2012). APPROACH was a continuous variable that measured whether an eagle was flying toward the nearest turbine (APPROACH = 1 as the maximum value) or away from the nearest turbine (APPROACH = –1 as the minimum value). NORTH was a continuous variable that measured whether a flight path was directed northward (NORTH = 1 as the maximum value) or southward (NORTH = –1 as the minimum value). EAST was a continuous variable that measured whether a flight path was directed eastward (EAST = 1 as the maximum value) or westward (EAST = −1 as the minimum value). For additional details about explanatory variables, see Rolek *et al.* (2022).

Model formulation

We briefly describe the aspects of Rolek *et al.*'s (2022) modelling framework that we used and below we highlight the differences between that past work and this effort. We used a hierarchical generalized linear model to evaluate the probability that flight segments entered the rotor-swept zone (Rolek *et al.* 2022). We allowed the probability of entry to decrease as distance from the nearest turbine increased (Rolek *et al.* 2022).

We used binary occupancy data ($z_{i,t}$) structured as a matrix with each flight path (i) as a row and 5-s time steps (t) as columns. These data described whether an eagle occupied the rotor-swept zone, where $z_{i,t} = 1$ indicates an occupied rotor-swept zone during a 5-s time step. We assigned a Bernoulli distribution to the initial probability of occupancy of the rotor-swept zone during the first time step ($t = 1$), $z_{i,1} \sim \text{Bernoulli}(\psi)$, and this probability was estimated by the model using the parameter ψ that was bound between zero and one. We estimated occupancy during subsequent time steps $t = \{2, 3, \ldots T_i\}$ using a first-order Markov process to account for temporal autocorrelation, thereby explicitly estimating dynamics (MacKenzie *et al.* 2003, Royle & Kéry 2007). Our focal parameter, the probability that an eagle entered the rotor-swept zone, was represented by a colonization parameter, γ, and the probability that an eagle remained within the rotor-swept zone was represented by the persistence parameter ϕ. Hereafter we refer to these parameters as the probabilities of entry and persistence, respectively.

We specified occupancy dynamics as

$$z_{i,t} \sim \text{Bernoulli}\left(\gamma_{i,t-1}\left(1-z_{i,t-1}\right) + \phi z_{i,t-1}\right) \quad (1)$$

To include an effect of distance, we included the probability of entry as a Gaussian kernel that decreased monotonically as Euclidean distance ($x_{i,t-1}$) increased (Clobert *et al.* 2012) from a flight path segment to the rotor-swept zone of the nearest wind turbine (Rolek *et al.* 2022). The y-intercept (ρ) was a parameter estimated by the model that represented the maximum probability of entry at distance equal to zero ($x_{i,t-1} = 0$). The distance scale parameter (σ) was estimated by the model and described the steepness of the monotonic decrease in the probability of entry as distance increased:

$$\gamma_{i,t-1} = \rho_{i,t-1} e^{-x^2_{i,t-1}/\sigma^2_{i,t-1}} \quad (2)$$

This model structure allowed inclusion of explanatory variables as covariates (w) of the distance scale parameter using a log-link function

$$\log\left(\sigma_{i,t-1}\right) = \log\left(\beta_{j,1}\right) + w_{2,i,t-1}\beta_{j,2} + \ldots + w_{N,i,t-1}\beta_{j,N} \quad (3)$$

Here, we specified explanatory variables as covariates including SPEED, APPROACH and a first-order interaction between SPEED and APPROACH. Doing this

meant that probability of entry could be estimated as a continuous slope estimate with a mean ($\beta_{j,1}$) that varies among turbines ($j = \{1, 2, 3 \ldots J\}$) and can range between a flat slope (greater values of σ, e.g. 500–3000) or a steeper slope (smaller values of σ, e.g. 0–100) as distance increases. The distance scale parameter can be assigned covariates, thereby influencing the magnitude of effect from distance on the probability of entry.

In past work (Rolek *et al.* 2022), we did not allow the effect of distance on probability of entry to vary among turbines. In this study, we allowed both probability of entry and the value of the coefficients of covariates to vary among turbines. We specified these coefficients to be governed by hyperparameters as $\mathbf{B} \sim$ multivariate normal $(\boldsymbol{\mu}, \boldsymbol{\Sigma})$, where $\mathbf{B}$ was a matrix of coefficient estimates (i.e. $\mathbf{B} = \beta_{1:J,1:N}$) that varied by turbine, and columns represented the number of hyperparameters ($n = 4$) included within the distance scale submodel. The hyperparameter $\boldsymbol{\mu}$ was a vector of means for each coefficient including the intercept and each covariate. The variance–covariance matrix ($\boldsymbol{\Sigma}$) included parameters representing the standard deviation (τ) for each hyperparameter. Correlation coefficients (η) explicitly estimated correlations between hyperparameters.

$$\boldsymbol{\Sigma} = \begin{pmatrix} \eta\tau_1\tau_1 & \cdots & \eta_{1,N}\tau_1\tau_N \\ \vdots & \ddots & \vdots \\ \eta_{1,N}\tau_{1,N}\tau_1 & \cdots & \eta_{N,N}\tau_N\tau_N \end{pmatrix}$$

This formulation allowed coefficients to vary among turbines, and estimates were partially pooled toward the hyperparameter mean of each coefficient. The amount of partial pooling for each turbine-varying coefficient depended on sample size (Gelman & Hill 2007) for each turbine.

Similarly, we included explanatory variables as covariates to the *y*-intercept that estimated the maximum probability of entry into the rotor-swept zone using the logit link function

$$\text{logit}\left(\rho_{i,t-1}\right) = \alpha_{j,1} + \mathrm{u}_{2,i,t-1}\alpha_{j,2} + \ldots + \mathrm{u}_{L,i,t-1}\alpha_{j,L} \quad (4)$$

The *y*-intercept governed the maximum probability of entry when distance equals zero. We allowed the maximum probability of entry ($\alpha_{j,1}$) to vary among turbines and coefficients of covariates varied among turbines ($\alpha_{j,2}$, $\alpha_{j,3}$, $\ldots$ $\alpha_{j,L}$).

The *y*-intercept included the covariates SPEED, APPROACH, NORTH and EAST. Additionally, we included ALTITUDE and ALTITUDE SQUARED as explanatory variables to allow a quadratic response by the probability of entry. We allowed first-order interactions between the covariates SPEED and APPROACH, as well as NORTH and EAST.

We assigned coefficients a multivariate normal distribution as $\mathbf{A} \sim$ multivariate normal $(\boldsymbol{\delta}, \boldsymbol{\Omega})$, where $\mathbf{A}$ was a matrix of coefficient estimates (i.e. $\mathbf{A} = \alpha_{1:J,1:L}$) that varied by turbine ($j = 1, 2, 3, \ldots J$) and columns represented the number of hyperparameters ($L = 9$) in the *y*-intercept submodel. A vector of hyperparameters, $\boldsymbol{\delta}$, estimated the mean of each coefficient for the intercept and covariates. The variance–covariance matrix ($\boldsymbol{\Omega}$) included parameters representing the standard deviation (ν) for each hyperparameter. Correlation coefficients (λ) explicitly estimated correlations between hyperparameters.

$$\boldsymbol{\Omega} = \begin{pmatrix} \lambda_1\nu_1\nu_1 & \cdots & \lambda_{1,L}\nu_1\nu_L \\ \vdots & \ddots & \vdots \\ \lambda_{1,L}\nu_{1,L}\nu_1 & \cdots & \lambda_{L,L}\nu_L\nu_L \end{pmatrix}$$

Coefficient estimates varied across turbines, and these estimates were partially pooled toward overall means (Gelman & Hill 2007). As in our previous work (Rolek *et al.* 2022) we refer to the *y*-intercept hereafter as 'apex entry' because it represents the greatest probability of entry while ignoring random effects. We refer to the distance scale parameter as 'flatness' because it is inversely related to the slope of the decrease in probability of entry with distance (Rolek *et al.* 2022). See glossary (Supporting Information Table S1) for definitions of other terms and parameters. We considered covariates to be associated with apex entry or flatness when 95% highest density intervals (HDIs) of their coefficients excluded zero. To determine whether a turbine was significantly different from the overall mean of each covariate, we calculated the difference between the posterior distribution of hyperparameter means from estimates of each turbine, and calculated the probability of direction (Makowski *et al.* 2019). We considered turbines significantly different from average when the probability of direction was ≥0.95.

Model implementation

We used statistical software R (R Core Team 2022) to implement models and estimate parameters with Bayesian Markov-Monte Carlo simulations using the NIMBLE package (NIMBLE Development Team 2019). We used three chains with 25 000 burn-in, and 25 000 posterior iterations with a thinning interval of 25 iterations. This implementation provided 3000 posterior draws (i.e. 1000 draws from each chain). We assessed convergence of chains using traceplots and the Gelman–Rubin diagnostic (Gelman & Rubin 1992), and we assigned adequate convergence when traceplots of parameters did not visually appear to drift and $\hat{R} \geq 1.1$.

Sample size

We retained data that included 13 419 flight paths, of which 2364 (18%) entered the rotor-swept zone. Identi-Flight recorded a mean of 7.1 segments (median = 5, range = 2–248) for each retained flight path. In total, flight paths included 95 182 segments for analysis, of which 5828 (16%) occupied the rotor-swept zone. Segments of eagle flight paths entered the rotor-swept zone 1457 times, persisted within the rotor-swept zones 3105 times and occupied the rotor-swept zone during the first segment 870 times. For additional details see Rolek *et al.* (2022).

RESULTS

Covariates associated with apex entry included APPROACH, ALTITUDE and ALTITUDE SQUARED (Table 1). These associations indicated a peak in probability of entry at 73.6 m in altitude (Fig. 1) and at angles directly approaching the turbines (Fig. 2). Therefore, eagles were most likely to enter rotor-swept zones when flying directly toward a turbine at roughly hub height.

The relationship of probability of entry with distance changed as a function of SPEED and APPROACH, with faster flying and more directly approaching eagles more likely to enter at greater distances (Fig. 3). Each of the relationships mentioned above varied per turbine such that some turbines were substantially more associated with covariates and others less so (Figs 1–3, Supporting Information Fig. S1).

We visually examined the spatial pattern of apex entry among turbines (Supporting Information Fig. S2).

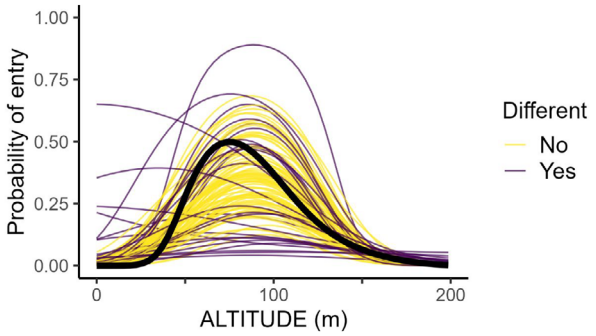

Figure 1. Associations between the probability of entering the rotor-swept zone in response to flight altitude of eagles (ALTITUDE) at Top of the World wind facility in Wyoming, USA. Thin lines depict means of individual turbines, and colours illustrate whether turbines were similar to the overall mean among turbines (yellow; Different = 'No') or had significant differences from the mean (purple; having a probability of direction ≥ 95%; Different = 'Yes'). Thick line depicts overall mean among turbines.

Table 1. Parameter estimates of the mean among turbines and 95% highest density intervals (95% LHDI and 95% UHDI). Covariates that are significantly different from no effect (zero) are indicated in bold.

Group	Parameter	Mean	95% LHDI	95% UHDI
Apex	INTERCEPT	−1.89	−2.07	−1.72
	SPEED	−0.11	−0.25	0.03
	APPROACH	**1.14**	**0.93**	**1.36**
	NORTH	0.01	−0.12	0.14
	EAST	0.05	−0.09	0.20
	SPEED: APPROACH	−0.20	−0.40	0.01
	NORTH:EAST	−0.01	−0.30	0.28
	ALTITIUDE	**−4.01**	**−4.55**	**−3.49**
	ALTITUDE SQUARED	**−4.05**	**−4.63**	**−3.49**
Flatness	INTERCEPT	3.67	3.59	3.75
	SPEED	**0.12**	**0.06**	**0.19**
	APPROACH	**0.14**	**0.05**	**0.23**
	SPEED: APPROACH	−0.05	−0.14	0.06

We did not detect any patterns or clumping of particularly safe or dangerous turbines but note that the turbines that differed from average occurred in the western portion of the study area. Future work might examine entry regarding topographical variables and landscape characteristics.

DISCUSSION

We have previously demonstrated that many eagles that triggered curtailments never entered the rotor-swept zone, and suggested that turbine-specific criteria could be developed to take into account the relative collision risk at a specific turbine (McClure *et al.* 2021a). The current study illustrates the potential value of turbine-specific curtailment criteria by demonstrating that flight characteristics associated with entry by eagles into the rotor-swept zones of wind turbines can vary among turbines. Curtailment criteria could therefore be designed to vary by turbine to account for specific flight characteristics that predict entry into the rotor-swept zone of a given turbine.

The existing curtailment regimen at Top of the World is reasonably suited to the average turbine, with three-dimensional distance from turbine predictive of eagle entry into the rotor-swept zone (Rolek *et al.* 2022). Our results suggest that entry into rotor-swept zones of some turbines is particularly associated with a specific set of flight characteristics. Entry for some turbines was associated with faster or slower flight

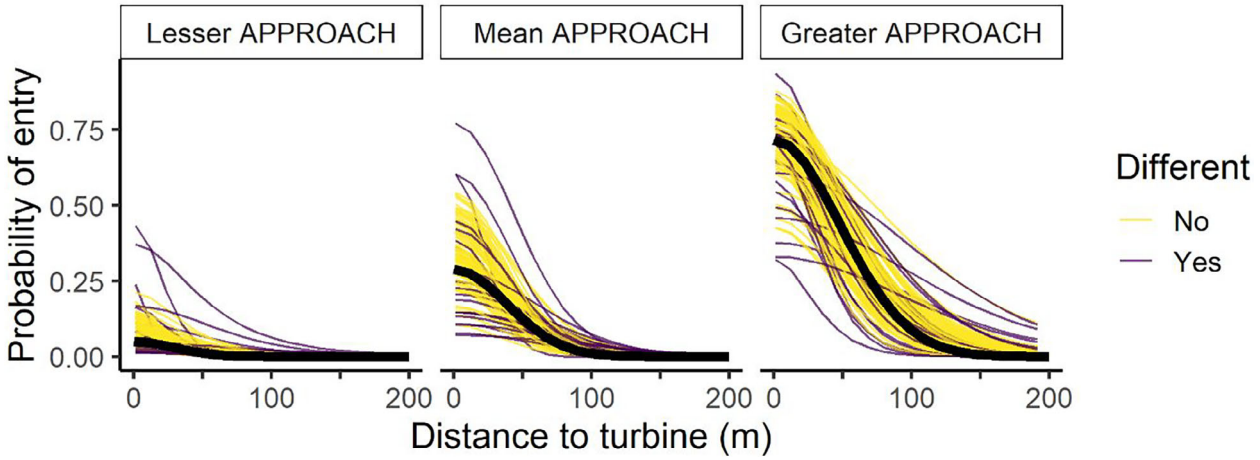

Figure 2. The probability of entering the rotor-swept zone (entry) in response to distance to nearest turbine and effects from APPROACH, at Top of the World wind facility in Wyoming, USA. APPROACH was a covariate that measured how much an eagle was flying toward the nearest turbine and was associated with both apex entry and flatness. Thin lines depict means of individual turbines, and colours depict whether turbines had significant differences from the overall mean among turbines (having a probability of direction ≥95%) for apex entry, flatness or response to APPROACH. Thick lines depict overall means among turbines. ALTITUDE is set to values where the apex probability of entry reaches its maximum value (ALTITUDE 73.6 m). 'Lesser', 'mean' and 'greater' APPROACH correspond to the minimum (i.e. −1), mean (i.e. 0) and maximum values (i.e. 1), respectively.

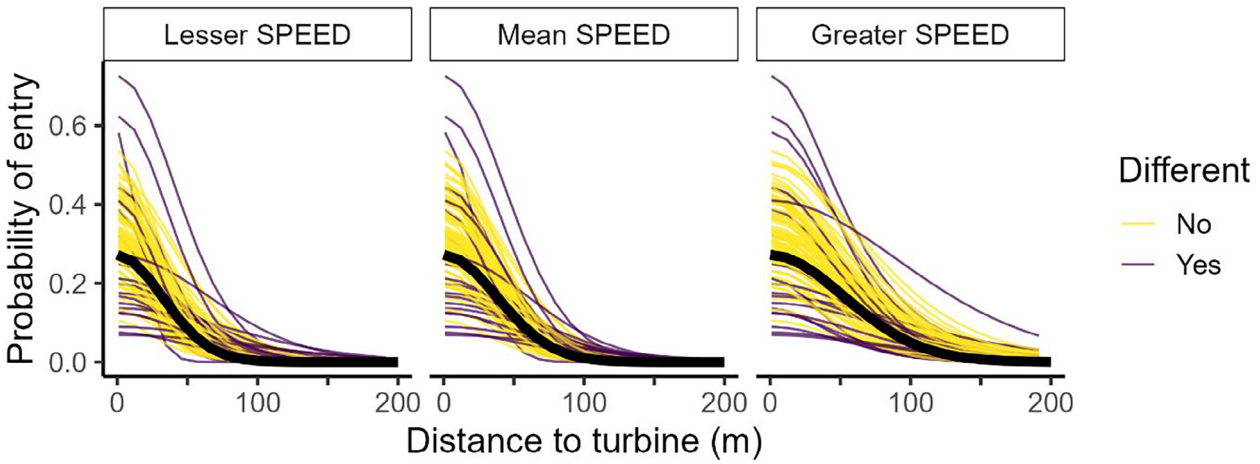

Figure 3. The probability of entering the rotor-swept zone (entry) in response to eagle speed (SPEED) and its effect on the flatness of response while increasing distance to the nearest turbine. Thin lines depict means of individual turbines, and colours depict whether turbines had significant differences from the overall mean among turbines (having a probability of direction ≥ 95%) for apex entry, flatness, or response to SPEED. Thick lines depict overall means among turbines. ALTITUDE is set to values where the apex probability of entry reaches its maximum value (ALTITUDE 73.6 m). 'Lesser' corresponds to 2.5 centiles of SPEED, and 'greater' corresponds to 97.5 centiles.

speeds, higher or lower flight altitudes, and closer or further distances from turbines. For example, we previously demonstrated that eagles are most likely to enter rotor-swept zones when flying near the hub height of turbines (Rolek *et al.* 2022). Although this relationship exists on average across turbines, entry into rotor-swept zones of some turbines is associated with lower flight altitudes (Fig. 1). Indeed, at some turbines we detected little relationship between entry into the rotor-swept zone and flight altitude (Fig. 1). Curtailment criteria might therefore be adjusted accordingly with the speed, distance and altitude at which shut-down occurs, reflecting the

most likely flight paths to enter the rotor-swept zone of a particular turbine.

It is important to interpret our results in the context in which our data were collected. For example, we examined the flight paths of eagles that triggered curtailment, but the act of curtailment itself may affect an eagle's flight behaviour. Further, the machine-vision system used at our study site had a false classification rate for non-eagles of 28% in a proof-of-performance test (McClure *et al.* 2018), and the classification algorithm appears not to have improved over time (Duerr *et al.* 2023). Some unknown proportion of the flight paths that we analysed were therefore of non-eagles. These birds presumably have different flight characteristics, and different probabilities of entry, as eagles, and these differences may affect our modelled results. Finally, the particular entry rates and their relationships with flight characteristics are site-specific and caution is warranted when applying our inference to other wind-power facilities. That said, our overall finding that the relationship between flight characteristics and rotor-swept entry varies per turbine probably applies to other wind-power facilities and may be related to topography surrounding a turbine or location of a turbine in a string (Smallwood *et al.* 2007). Indeed, the drastic differences in turbine-specific predictors of rotor-swept zone entry suggest that each wind-power facility implementing automated curtailment might be able to consider tailoring curtailment criteria to each turbine.

Automated curtailment has potential to reduce fatalities of target species at wind-power facilities. However, this mitigation option is not a panacea (McClure *et al.* 2021b) and it is unlikely to eliminate fatalities of all species or even focal species. As currently implemented, automated curtailment substantially increases the number of curtailments relative to curtailment operated by human observers (McClure *et al.* 2021b). Customizing the curtailment algorithm to each turbine might lessen fatalities of target species while also reducing impacts to energy production. Such adjustments could increase the efficacy of wind power, allowing it to meet more effectively the mandated standards associated with reduction in the use of fossil fuels.

The Research Computing Team at Boise State University provided technical assistance. Taber Allison, Stu Webster, Juan Botero, Isabel Gottlieb, Will Vesely, Tom Hiester, Carlos Jorquera, Tyler Derritt, Greg Aldrich and Tim Hayes provided logistical support. Any use of trade, firm or product names is for descriptive purposes only and does not imply endorsement by the U.S. Government. The Renewable Energy Wildlife Research Fund, the MJ Murdock Charitable Trust and the author's institutions funded this work. We also thank reviewers and editors for their constructive comments.

AUTHOR CONTRIBUTIONS

Brian W. Rolek: Methodology; formal analysis; data curation; Writing- Original draft; Visualization. **Melissa A. Braham:** Data curation; methodology; Writing- Review & Editing. **Tricia A. Miller**: Methodology; Writing- Review & Editing. **Adam E. Duerr:** Methodology; Writing- Review & Editing. **Todd E. Katzner:** Methodology; supervision; Writing- Review & Editing. **Christopher J. W. McClure:** Methodology; Writing- Original draft.

CONFLICT OF INTEREST STATEMENT

The authors declare that they have no conflicts of interest.

FUNDING

Renewable energy wildlife institute.

Data Availability Statement

This study uses the same data as Rolek *et al.* (2022), which are available as supplementary data Appendix S1 to that study.

ETHICAL NOTE

None.

REFERENCES

Allison, T.D., Cochrane, J.F., Lonsdorf, E. & Sanders-Reed, C. 2017. A review of options for mitigating take of Golden eagles at wind energy facilities. *J. Raptor Res.* **51**: 319–333.

BirdLife International. 2015. *Review and Guidance on Use of "Shutdown-on-Demand" for Wind Turbines to Conserve Migration Soaring Birds in the Rift Valley/Red Sea Flyway*.

Clobert, J., Baguette, M., Benton, T.G. & Bullock, J.M. 2012. *Dispersal Ecology and Evolution*. Oxford: Oxford University Press.

Crawley, M.J. 2012. *The R Book*. Chichester: John Wiley & Sons.

De Lucas, M., Janss, G.F.E., Whitfield, D.P. & Ferrer, M. 2008. Collision fatality of raptors in wind farms does not depend on raptor abundance. *J. Appl. Ecol.* **45**: 1695–1703.

De Lucas, M., Ferrer, M., Bechard, M.J. & Muñoz, A.R. 2012. Griffon vulture mortality at wind farms in southern Spain: Distribution of fatalities and active mitigation measures. *Biol. Conserv.* **147**: 184–189.

Duerr, A.E., Parsons, A.E., Nagy, L.R., Kuehn, M.J. & Bloom, P.H. 2023. Effectiveness of an artificial intelligence-based system to curtail wind turbines to reduce eagle collisions. *PloS One* **18**: e0278754.

Gelman, A. & Hill, J. 2007. *Data Analysis Using Regression and Multilevel/Hierarchical Models*. New York, NY: Cambridge University Press.

Gelman, A. & Rubin, D.B. 1992. Inference from iterative simulation using multiple sequences. *Stat. Sci.* **7**: 457–472.

MacKenzie, D.I., Nichols, J.D., Hines, J.E., Knutson, M.G. & Franklin, A.B. 2003. Estimating site occupancy, colonization, and local extinction when a species is detected imperfectly. *Ecology* **84**: 2200–2207.

Makowski, D., Ben-Shachar, M.S. & Lüdecke, D. 2019. bayestestR: Describing effects and their uncertainty, existence and significance within the Bayesian framework. *J. Open Source Softw.* **4**: 1541.

Marques, A.T., Batalha, H., Rodrigues, S., Costa, H., Pereira, M.J.R., Fonseca, C., Mascarenhas, M. & Bernardino, J. 2014. Understanding bird collisions at wind farms: An updated review on the causes and possible mitigation strategies. *Biol. Conserv.* **179**: 40–52.

McClure, C.J.W., Martinson, L. & Allison, T.D. 2018. Automated monitoring for birds in flight: Proof of concept with eagles at a wind power facility. *Biol. Conserv.* **224**: 26–33.

McClure, C.J.W., Rolek, B.W., Braham, M.A., Miller, T.A., Duerr, A.E., McCabe, J.D., Dunn, L. & Katzner, T.E. 2021a. Eagles enter rotor-swept zones of wind turbines at rates that vary per turbine. *Ecol. Evol.* **11**: 11267–11274.

McClure, C.J.W., Rolek, B.W., Dunn, L., McCabe, J.D., Martinson, L. & Katzner, T.E. 2021b. Eagle fatalities are reduced by automated curtailment of wind turbines. *J. Appl. Ecol.* **58**: 446–452.

McClure, C.J.W., Rolek, B.W., Dunn, L., McCabe, J.D., Martinson, L. & Katzner, T.E. 2022. Confirmation that eagle fatalities can be reduced by automated curtailment of wind turbines. *Ecol. Solut. Evid.* **3**: e12173.

NIMBLE Development Team. 2019. *NIMBLE: MCMC, Ecological Solutions and Evidence*.

Perold, V., Ralston-Paton, S. & Ryan, P. 2020. On a collision course? The large diversity of birds killed by wind turbines in South Africa. *Ostrich* **91**: 228–239.

R Core Team 2022. *R: A Language and Environment for Statistical Computing*. Vienna: R Foundation for Statistical Computing.

Rolek, B.W., Braham, M.A., Miller, T.A., Duerr, A.E., Katzner, T.E., McCabe, J.D., Dunn, L. & McClure, C.J.W. 2022. Flight characteristics forecast entry by eagles into rotor-swept zones of wind turbines. *Ibis* **164**: 1–13.

Royle, J.A. & Kéry, M. 2007. A Bayesian state-space formulation of dynamic occupancy models. *Ecology* **88**: 1813–1823.

Smallwood, K.S., Thelander, C.G., Morrison, M.L. & Rugge, L.M. 2007. Burrowing owl mortality in the Altamont pass wind resource area. *J. Wildl. Manage.* **71**: 1513–1524.

Received 11 April 2023;
Revision 26 July 2023;
revision accepted 31 July 2023.
Associate Editor: Kurt Burnham.

SUPPORTING INFORMATION

Additional supporting information may be found online in the Supporting Information section at the end of the article.

Figure S1. Density plots of draws from posterior distributions of coefficients for covariates. Each curve represents density of model-estimated values for an individual turbine.

Figure S2. Model estimated means and standard deviations (SDs) for apex intercept for each turbine while holding all other covariates to their means. The *x*-axis is longitude and the *y*-axis is latitude.

Table S1. Glossary.